Observation of forbidden transitions of ammonium ion (NH_4^+) ν_3 band and determination of ground state rotational constants. Observation of ν_3 band allowed transitions of ND_4^+

Mark W. Crofton and Takeshi Oka
Department of Chemistry and Department of Astronomy and Astrophysics, The University of Chicago, Chicago, Illinois 60637

(Received 9 December 1986; accepted 29 January 1987)

The high resolution infrared spectrum of forbidden transitions of the ν_3 band of ammonium ion, NH_4^+, has been recorded using a difference frequency spectrometer. These are the first forbidden NH_4^+ lines to be observed. For $5 \leqslant R \leqslant 11$, 24 forbidden transitions have been assigned. From combination difference relations involving the same excited state level, 13 independent energy differences between ground state levels with $4 \leqslant J \leqslant 11$ have been determined with uncertainties of $\lesssim 0.004$ cm^{-1}. From this data, the following values (in cm^{-1}) for ground state constants of NH_4^+ have been determined ($\pm 3\sigma$): $B = 5.929\,32 \pm 0.000\,20$, $D = (-1.282 \pm 0.020) \times 10^{-4}$, and $D_t = (4.80 \pm 0.35) \times 10^{-6}$. The value of r_0 is calculated to be $1.028\,73 \pm 0.000\,02$ Å, while r_e is estimated to be 1.0208 ± 0.0020 Å. More than 100 transitions of the ν_3 band of ND_4^+ were also observed ($J \lesssim 10$) by the same spectrometer. Nearly all of these have been assigned and fit together using a linear model. A determination of B_0 for ND_4^+, while unsuccessful at this time, will allow a more accurate determination of r_e.

I. INTRODUCTION

Recent observations[1,2] of the high resolution infrared spectrum of the ν_3 band of the ammonium ion NH_4^+ have given the first experimental information for the molecular structure of this well-known ion in the free gaseous state. The structure was clearly shown to be tetrahedral as expected and the equilibrium bond length was estimated[1] to be 1.026 ± 0.005 Å. Because of the nature of the infrared transition involving a triply degenerate vibrational state, however, it was not possible to obtain the experimental value of the ground state rotational constant B_0 which is needed for the structural determination. The value of B_0 was derived using an assumed value of the Coriolis coupling constant ζ_3 and thus had a large uncertainty. More extensive observation and analysis of the ν_3 band by Schafer, Saykally, and Robiette[3] has led to more detailed information on vibration–rotation interactions but did not help this situation. In order to determine the ground state rotational constants experimentally, it is imperative to observe forbidden transitions for which $\Delta R \neq 0$. Such transitions are weaker than the allowed transitions typically by two orders of magnitude and thus it was difficult to observe and definitely assign these transitions. More recently Nakanaga and Amano[4] have observed the ν_4 fundamental band of monodeuterated ammonium ion NH_3D^+ and determined the ground state rotational constant B_0 of this species. By assuming the variation α of the rotational constant B upon vibrational excitation to be identical between NH_3D^+ and CH_3D, they have estimated the NH bond length to be 1.020 Å which agrees well with the theoretical prediction by Yamaguchi and Schaefer,[5] 1.0215 Å.

In this paper we report our observation of forbidden transitions in the ν_3 band of NH_4^+ which give us directly the experimental values of ground state rotational constants. This was made possible by the recent increase in sensitivity of our infrared spectrometer. The forbidden transitions are observed with sufficient signal-to-noise ratio to allow 24 of them to be easily observed and assigned. When combined with our previous measurement of allowed transitions, these provided enough ground state combination differences to enable an accurate determination of B_0, D_0, and D_t. The value of B_0 gives us immediately the r_0 bond length. In order to obtain the equilibrium bond length r_e, however, we need additional information. The observation of the ν_3 band of ND_4^+ was attempted in part for this purpose. The allowed transitions of this band have been observed with signal-to-noise ratio ~ 100 for the strongest, but the forbidden transitions are expected to be at least one order of magnitude weaker relative to those for NH_4^+ and were not observable.

II. EXPERIMENTAL

A difference frequency laser system[6] was employed for the observation of the NH_4^+ and ND_4^+ infrared spectra, as we did for our initial observation[1] of the ν_3 band of NH_4^+. The cw radiations of an Ar ion laser and a ring dye laser are mixed in a $LiNbO_3$ crystal which generates the difference frequency in the infrared. By tuning the crystal temperature and dye laser frequency, continuously tunable infrared laser radiation is generated in the region 2300–4500 cm^{-1}. With typical input power levels of 400 mW in each of the visible lasers, $\sim 20\,\mu$W of IR is available for absorption spectroscopy of NH_4^+ and ND_4^+ ν_3 bands. About 10% of this radiation is split off and used to record the spectrum of a standard gas, NH_3[7] or N_2O[8] in this case, for frequency calibration purposes. As usual, the remainder is split equally into two beams, one for noise reference and the other for the ion sig-

 0021-9606/87/115983-06$02.10

nal. Each of these is focused onto an InSb photovoltaic infrared detector element at 77 K and the resulting signals are combined 180° out of phase to subtract the noise component. This "noise subtraction"[9] reduces the noise level typically by a factor of 20, since the amplitude noise of the infrared source dominates other noise sources before subtraction. In order to increase the absorption path length, the infrared beam is sent four times unidirectionally through the cell containing the ions. These noise reduction and signal enhancing techniques were essential for the observation and analysis of NH_4^+ ν_3 band forbidden transitions. The strongest forbidden transition line has a signal-to-noise ratio of only ~ 15, being ~ 50 times weaker than the strongest allowed transition.

The ions were generated in a water cooled glass cell of 80 cm length and 12 mm bore with multiple inlet and outlet ports in a symmetrical configuration. A 6 kHz glow discharge was run in this cell through H_2/NH_3 or D_2/ND_3 at a ratio of 10:1 and total pressure of 1.2 Torr. Discharges were also done in $He/H_2/NH_3$ and $He/D_2/ND_3$ (150:3:2) at a total pressure of 7 Torr with slightly reduced NH_4^+/ND_4^+ signals. The latter discharge was useful in conserving the relatively expensive D_2 and ND_3. In the He/H_2 discharge with reduced NH_3, many additional ion lines were observed for which the carrier is unknown. The analysis of these should prove to be very interesting.

Detection of the ion transitions, in any case, was done by looking for velocity modulated[10] signals in a narrow bandwidth about the 6 kHz discharge frequency. Thus, our experimental setup was virtually identical to what we have used for other recent infrared spectroscopic studies of ions.[11,12] The entire spectrum was very nearly free of all neutral absorption features, because of the high symmetry of the discharge cell. Only the strongest NH_3 lines were present at all as small humps, easily distinguishable from genuine ion lines.

III. ANALYSIS

A. Forbidden transitions of NH_4^+

A total of 24 forbidden transitions ($\Delta R = \pm 1$) of the NH_4^+ ν_3 band have been observed and assigned for $5 \leqslant R \leqslant 11$, and are listed in Table I together with allowed transitions used for combination difference purposes. We have used our own measurements of allowed transition frequencies rather than those of Schäfer *et al.*[3] for greater consistency and probable higher accuracy. The 24 assigned lines represent most of the observable forbidden lines at the existing discharge temperature. Some of the transitions for higher quantum states would have been observable as well as a few more of the lower J transitions but were not searched for. It would be difficult to extend the observation of R branch lines further to the blue, since the infrared power level falls off in the region of 3500 cm^{-1} and lowers the sensitivity.

The assignments of forbidden lines were made with the aid of the frequency and intensity predictions resulting from Robiette's fitting of extensive data[3] on ν_3 band allowed transitions with assumed ground state constants. These predictions could not be made with high absolute accuracy because constants such as B_3, B_0, ν_0, and ζ_3 are not separately deter-

TABLE I. NH_4^+ ν_3 band forbidden transitions and allowed transitions with common upper state.

Forbidden transition		Frequency[a]	Allowed transition		Frequency[a]
$P0(9)$	$A2(1)$–$A1(1)$	3231.419	$Q0(8)$	$A2(1)$–$A1(1)$	3337.862[b]
$P0(9)$	$F2(1)$–$F1(2)$	3231.478	$Q0(8)$	$F2(1)$–$F1(1)$	3337.889[b]
$P0(8)$	$F1(1)$–$F2(1)$	3244.304	$Q0(7)$	$F1(1)$–$F2(1)$	3338.939
$P0(7)$	$F1(1)$–$F2(2)$	3256.979	$Q0(6)$	$F1(1)$–$F2(1)$	3339.843
$P0(7)$	$A1(1)$–$A2(1)$	3257.086	$Q0(6)$	$A1(1)$–$A2(1)$	3339.930[b]
$P0(6)$	$F1(1)$–$F2(2)$	3269.665	$Q0(5)$	$F1(1)$–$F2(1)$	3340.720
$Q+(5)$	$F1(2)$–$F2(1)$	3345.177	$P+(6)$	$F1(2)$–$F2(2)$	3274.123
$Q+(9)$	$A2(1)$–$A1(1)$	3345.279	$P+(10)$	$A2(1)$–$A1(1)$	3227.193
$Q+(8)$	$A2(1)$–$A1(1)$	3345.306[b]	$P+(9)$	$A2(1)$–$A1(1)$	3238.857
$Q+(6)$	$F1(2)$–$F2(1)$	3345.313[b]	$P+(7)$	$F1(2)$–$F2(2)$	3262.453
$Q+(7)$	$F2(2)$–$F1(1)$	3345.313[b]	$P+(8)$	$F2(2)$–$F1(2)$	3250.654
$Q+(6)$	$A1(1)$–$A2(1)$	3345.557	$P+(7)$	$A1(1)$–$A2(1)$	3262.711
$Q+(7)$	$F1(1)$–$F2(1)$	3345.658[b]	$P+(8)$	$F1(1)$–$F2(1)$	3251.015
$Q+(8)$	$F2(2)$–$F1(1)$	3345.658[b]	$P+(9)$	$F2(2)$–$F1(2)$	3239.252
$Q+(8)$	$E(1)$–$E(1)$	3345.727	$P+(9)$	$E(1)$–$E(1)$	3239.324
$Q+(9)$	$F1(2)$–$F2(1)$	3345.747	$P+(10)$	$F1(2)$–$F2(2)$	3227.595
$Q+(10)$	$A1(1)$–$A2(1)$	3345.774	$P+(11)$	$A1(1)$–$A2(1)$	3215.912
$R+(4)$	$A2(1)$–$A1(1)$	3404.129	$P+(6)$	$A2(1)$–$A1(1)$	3273.836
$R0(5)$	$F1(2)$–$F2(1)$	3411.813	$Q0(6)$	$F1(2)$–$F2(2)$	3340.758
$R0(6)$	$A1(1)$–$A2(1)$	3422.796	$Q0(7)$	$A1(1)$–$A2(1)$	3339.950[b]
$R0(7)$	$F1(1)$–$F2(1)$	3433.843	$Q0(8)$	$F1(1)$–$F2(1)$	3339.200[b]
$R0(7)$	$F2(2)$–$F1(1)$	3434.080	$Q0(8)$	$F2(2)$–$F1(2)$	3339.412
$R+(7)$	$A1(1)$–$A2(1)$	3439.402	$P+(9)$	$A1(1)$–$A2(1)$	3238.364
$R0(8)$	$A2(1)$–$A1(1)$	3444.993	$Q0(9)$	$A2(1)$–$A1(1)$	3338.550

[a] In cm^{-1} units.
[b] Blended transition.

minable from the allowed data set. Only combinations of these constants such as $B_3 - B_0$, $\nu_0 - 2B_3\zeta_3$, and $B_3 - B_3\zeta_3$ can be determined. If any one of these parameters is determined, however, obviously the rest are also determined. The relative spacings of any set of forbidden lines with same values of R can be well predicted. This is because the difference in fine structure splitting between lower and upper states is known from allowed transitions. The magnitude of the Coriolis splitting in the excited state was not known precisely because $B_3\zeta_3$ was not known precisely. The error in $B_3\zeta_3$ produced the large error in the prediction of forbidden transition frequencies. Figure 1 shows an energy diagram for some upper and lower state energy levels and indicates the allowed and forbidden transitions between these levels. In our earlier work[1] we estimated the value of ζ_3 to be 0.048 ± 0.005. This value was also used for the prediction of forbidden line frequencies and intensities.[3] The error in ζ_3 is large, leading to typical errors in frequency predictions of more than 1 cm^{-1}. The intensities of forbidden transitions relative to each other were approximately correct. Intensities of forbidden lines relative to allowed lines were overestimated by a factor of 2–3. This is at least partially due to our underestimate of ζ_3. Such an underestimate leads to a small Coriolis splitting in the excited state, resulting in overestimated mixing between levels of same J but with R differing by one. It is this mixing which gives intensity to the forbidden transitions. Since the value of ζ_3 in CD_4 is 0.160,[13] we can expect that observation of ND_4^+ forbidden lines by our spectrometer will have to wait for a sensitivity improvement. The value of B_0 for CD_4 was determined initially by Raman spectroscopy[14,15] because conventional infrared absorption was not sensitive enough.

The new data, when combined with measurements of allowed transitions, allows the separation of ν_0, B_3, $B_3\zeta_3$,

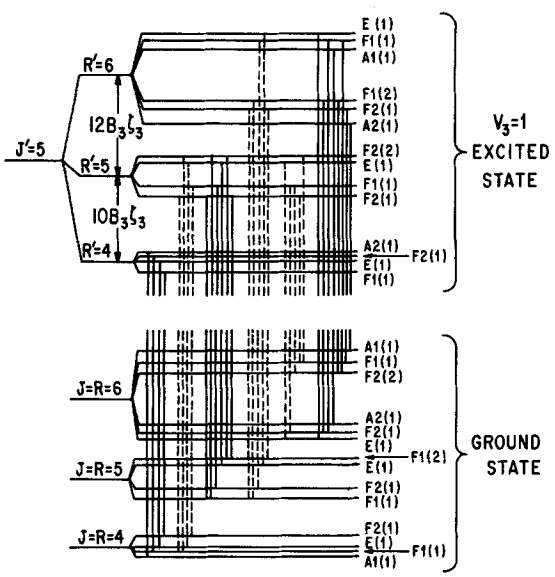

FIG. 1. Energy level diagram showing transitions to $J' = 5$ for the ν_3 band of NH_4^+/ND_4^+. The fine structure splittings within each state have been drawn to scale, but are uniformly exaggerated for the ground state. Forbidden transitions are indicated by dashed lines, allowed transitions by solid lines. Only the transitions R-(4), $R0(4)$, $Q0(5)$, $Q+(5)$, $P0(6)$, and $P+(6)$ are shown.

TABLE II. NH_4^+ ground state combination differences.

Upper level–lower level	Energy difference[a]	Obs − calc[b] ($\times 10^3$)
$11A2(1)$–$10A2(1)$	129.862	1
$10F2(2)$–$9F2(1)$	118.152	2
$10A1(1)$–$9A1(1)$	118.086	−1
$9A1(1)$–$8A1(1)$	106.444	−1
$9F1(2)$–$8F1(1)$	106.411	−2
$9E(1)$–$8E(1)$	106.403	−2
$9A2(1)$–$7A2(1)$	201.038	0
$8F1(2)$–$7F1(1)$	94.665	3
$8F2(1)$–$7F2(1)$	94.639	1
$7F2(2)$–$6F2(1)$	82.862	−2
$7A2(1)$–$6A2(1)$	82.846	−1
$6F2(2)$–$5F2(1)$	71.055	1
$6A1(1)$–$4A1(1)$	130.293	1

[a] In cm^{-1} units.
[b] Residuals are listed in units of 10^{-3} cm^{-1}.

and B_0. The use of combination difference relations with a common excited state level produced 13 independent energy differences between ground state levels. These are listed in Table II. In cases where the data yielded more than one ground state combination difference for the same ground state levels, a weighted average was taken, based on the estimated relative precision of the values. The uncertainties of the combination differences are $\lesssim 0.004$ cm^{-1} except in cases where the combination difference involved a blended transition or an exceptionally weak forbidden transition. The differences were fit using the following expression[16,23] for the energies of individual ground state levels of tetrahedral molecules:

$$W = BJ(J+1) - DJ^2(J+1)^2 + D_T f(J,\kappa) .$$

D_T is the quartic tensor centrifugal distortion constant, the lowest order ground state tetrahedral splitting parameter. The eigenvalues of the tetrahedral splitting $f(J,\kappa)$ have been tabulated.[16,23] Higher order centrifugal distortion constants and tensor terms were found to be indeterminable from the data set and unnecessary to fit the data to within experimental accuracy. They were therefore neglected in the fitting. Nevertheless, these higher order parameters, if similar to those of CH_4,[17,18] will begin to have a measurable effect on the transition frequencies for $J \sim 10$. Their absence in the fitting may produce slight errors in the values of the lower order parameters determined by the fit. Each ground state combination difference was weighted according to its estimated precision. The factors considered for the estimate of the precision included signal-to-noise ratios as well as number and agreement of combination differences for the same ground state levels. The weighting factors varied by no more than a factor of 10. The resulting values of ground state constants together with derived constants are listed in Table III.

In our previous work[1] we attempted to estimate ζ_3 for NH_4^+ by applying a mass only correction[19] to the value of ζ_3 for CH_4. This assumption that changes in the force constants could be ignored is a poor one, as is shown by the fact that the true correction to ζ_3 is of opposite sign to the mass correction.

The result $r_e = 1.0208$ Å was obtained by assuming the

TABLE III. NH_4^+ molecular constants.

	Ground state constants	
B	5.929 32(20)[a] cm^{-1} r_0	1.028 73(2) Å
D	$-1.282(20)\times10^{-4}$ cm^{-1} r_e	1.020 8(20)[b] Å
D_t	$4.80(35)\times10^{-6}$ cm^{-1}	
	Derived $V_3=1$ constants	
B_3	5.876 4(6)[c] cm^{-1}	5.879 4(12)[d] cm^{-1}
ζ_3	0.060 38(11)[c]	0.060 52(30)[d]

[a] Numbers in parentheses represent three standard deviations.
[b] This value of 3σ is an estimate.
[c] Obtained using parameters given in Ref. 3.
[d] Obtained using parameters given in Ref. 1.

same $r_0 - r_e$ as for CH_4,[20–22] but scaled to the ratio of the values of r_0. We expect this number to be accurate to $\pm$ 0.002 Å. It agrees very well with the *ab initio* equilibrium structure result[5] $r_e = 1.0215$ Å and with Nakanaga's and Amano's estimate[4] of 1.020 Å which is based on B_0 of NH_3D^+ and a similar type of assumption.

B. The ν_3 band of ND_4^+

The spectroscopy of the ν_3 band of ND_4^+ was quite straightforward. Figure 2 shows an experimental trace of $P+(9)$. A total of 123 transitions, listed in Table IV, were assigned and fit for $J'' \leqslant 9$. Unlike the case of NH_4^+, off-diagonal corrections to the energies of the excited state levels are very small. As a result, all transitions for $J'' \leqslant 9$ could be fit using a purely linear model. If one includes $J = 10$ lines in the fit, however, the residuals now become larger than the experimental uncertainty. This probably means that above $J = 9$ the linear model is no longer adequate. The ro-vibrational energy levels of the ν_3 state were expressed as

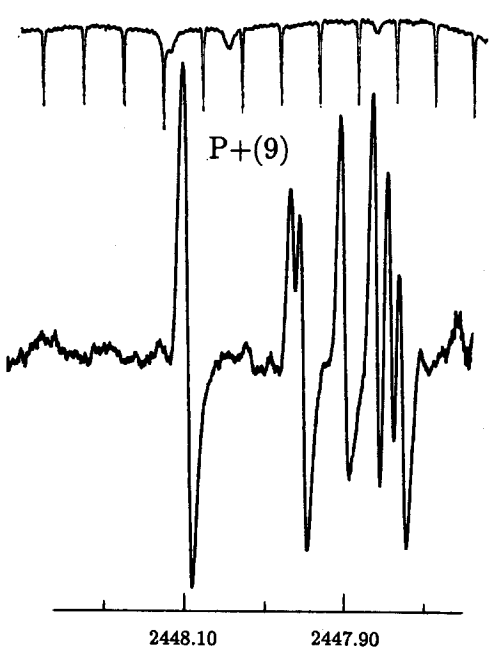

FIG. 2. The $P^+(9)$ transitions of ND_4^+. The upper trace is an N_2O spectrum for frequency calibration.

TABLE IV. The ν_3 band of ND_4^+.

Transition		Frequency (cm^{-1})	Obs − calc[a]
$P+(9)$	$A1(1)$–$A2(1)$	2447.828	0
$P+(9)$	$F1(2)$–$F2(2)$	2447.842	−1
$P+(9)$	$F2(3)$–$F1(3)$	2447.861	0
$P+(9)$	$A2(1)$–$A1(1)$	2447.903	−2
$P+(9)$	$F2(2)$–$F1(2)$	2447.952	2
$P+(9)$	$E(1)$–$E(1)$	2447.965[b]	3
$P+(9)$	$F1(1)$–$F2(1)$	2448.105[b]	0
$P+(9)$	$F2(1)$–$F1(1)$	2448.105[b]	−6
$P+(8)$	$F1(2)$–$F2(2)$	2453.083	−2
$P+(8)$	$E(2)$–$E(2)$	2453.099	2
$P+(8)$	$F2(2)$–$F1(2)$	2453.135	0
$P+(8)$	$F1(1)$–$F2(1)$	2453.179	1
$P+(8)$	$E(1)$–$E(1)$	2453.296[b]	3
$P+(8)$	$F2(1)$–$F1(1)$	2453.296[b]	−2
$P+(8)$	$A2(1)$–$A1(1)$	2453.296[b]	−9
$P+(7)$	$F2(2)$–$F1(2)$	2458.306	0
$P+(7)$	$E(1)$–$E(1)$	2458.332	1
$P+(7)$	$F1(2)$–$F2(2)$	2458.350	2
$P+(7)$	$A1(1)$–$A2(1)$	2458.384	5
$P+(7)$	$F1(1)$–$F2(1)$	2458.463	1
$P+(7)$	$F2(1)$–$F1(1)$	2458.473	0
$P+(6)$	$A2(1)$–$A1(1)$	2463.490	−4
$P+(6)$	$F2(1)$–$F1(1)$	2463.508	−2
$P+(6)$	$F1(2)$–$F2(2)$	2463.527	−2
$P+(6)$	$A1(1)$–$A2(1)$	2463.595	−4
$P+(6)$	$F1(1)$–$F2(1)$	2463.618[b]	0
$P+(6)$	$E(1)$–$E(1)$	2463.618[b]	−7
$P+(5)$	$F2(2)$–$F1(2)$	2468.669	1
$P+(5)$	$E(1)$–$E(1)$	2468.679	1
$P+(5)$	$F1(1)$–$F2(1)$	2468.738	4
$P+(5)$	$F2(2)$–$F1(1)$	2468.759	4
$P+(4)$	$F1(1)$–$F2(1)$	2473.800	−1
$P+(4)$	$E(1)$–$E(1)$	2473.841	2
$P+(4)$	$F2(1)$–$F1(1)$	2473.853	1
$P+(4)$	$A2(1)$–$A1(1)$	2473.871	1
$P+(3)$	$A1(1)$–$A2(1)$	2478.901	0
$P+(3)$	$F1(1)$–$F2(1)$	2478.925	1
$P+(3)$	$F2(1)$–$F1(1)$	2478.945	2
$P+(2)$	$F1(1)$–$F2(1)$	2483.986	−5
$P+(2)$	$E(1)$–$E(1)$	2484.002	−1
$Q0(9)$	$F2(1)$–$F1(1)$	2492.281	4
$Q0(9)$	$F1(1)$–$F2(1)$	2492.291	4
$Q0(9)$	$E(1)$–$E(1)$	2492.522	0
$Q0(9)$	$F2(2)$–$F1(2)$	2492.540	−1
$Q0(9)$	$A2(1)$–$A1(1)$	2492.616	0
$Q0(8)$	$A2(1)$–$A1(1)$	2492.633[b]	−2
$Q0(8)$	$F2(1)$–$F1(1)$	2492.647[b]	0
$Q0(8)$	$E(1)$–$E(1)$	2492.647[b]	−7
$Q0(9)$	$F2(3)$–$F1(3)$	2492.688	0
$Q0(9)$	$F1(2)$–$F2(2)$	2492.718	0
$Q0(9)$	$A1(1)$–$A2(1)$	2492.741	0
$Q0(8)$	$F1(1)$–$F2(1)$	2492.840	−1
$Q0(8)$	$F2(1)$–$F1(2)$	2492.910	−1
$Q0(7)$	$F2(1)$–$F1(1)$	2492.957	−4
$Q0(8)$	$E(2)$–$E(2)$	2492.973[b]	1
$Q0(7)$	$F1(1)$–$F2(1)$	2492.973[b]	−5
$Q0(8)$	$F1(2)$–$F2(2)$	2492.991	1
$Q0(7)$	$A1(1)$–$A2(1)$	2493.109	−1
$Q0(7)$	$F1(2)$–$F2(2)$	2493.159	0
$Q0(7)$	$E(1)$–$E(1)$	2493.186	1
$Q0(7)$	$F2(2)$–$F1(2)$	2493.226	0
$Q0(6)$	$E(1)$–$E(1)$	2493.243[b]	6
$Q0(6)$	$F1(1)$–$F2(1)$	2493.243[b]	−5
$Q0(6)$	$A1(1)$–$A2(1)$	2493.273	−5
$Q0(6)$	$F1(2)$–$F2(2)$	2493.385	0
$Q0(6)$	$F2(1)$–$F1(1)$	2493.416	2
$Q0(6)$	$A2(1)$–$A1(1)$	2493.442	3
$Q0(5)$	$F2(1)$–$F1(1)$	2493.472	1
$Q0(5)$	$F1(1)$–$F2(1)$	2493.502	−1

TABLE IV (*continued*).

Transition		Frequency (cm^{-1})	Obs − calc[a]
$Q0(5)$	$E(1)$–$E(1)$	2493.583	−2
$Q0(5)$	$F2(2)$–$F1(2)$	2493.598	−2
$Q0(4)$	$A2(1)$–$A1(1)$	2493.652	−3
$Q0(4)$	$F2(1)$–$F1(1)$	2493.677	−3
$Q0(4)$	$E(1)$–$E(1)$	2493.696	−1
$Q0(4)$	$F1(1)$–$F2(1)$	2493.749	−1
$Q0(3)$	$F2(1)$–$F1(1)$	2493.821	−1
$Q0(3)$	$F1(1)$–$F2(1)$	2493.846	1
$Q0(3)$	$A1(1)$–$A2(1)$	2493.876	1
$Q0(2)$	$E(1)$–$E(1)$	2493.935[b]	1
$Q0(2)$	$F1(1)$–$F2(1)$	2493.949[b]	4
$Q0(1)$	$F2(1)$–$F1(1)$	2494.010	2
$R-(0)$	$A2(1)$–$A1(1)$	2499.022	2
$R-(1)$	$F2(1)$–$F1(1)$	2503.968	1
$R-(2)$	$F1(1)$–$F2(1)$	2508.887[b]	6
$R-(2)$	$E(1)$–$E(1)$	2508.887[b]	3
$R-(3)$	$A1(1)$–$A2(1)$	2513.756[b]	2
$R-(3)$	$F1(1)$–$F2(1)$	2513.766[b]	3
$R-(3)$	$F2(1)$–$F1(1)$	2513.766[b]	−5
$R-(4)$	$F1(1)$–$F2(1)$	2518.598	−1
$R-(4)$	$E(1)$–$E(1)$	2518.623[b]	5
$R-(4)$	$F2(1)$–$F1(1)$	2518.623[b]	−1
$R-(4)$	$A2(1)$–$A1(1)$	2518.632[b]	−1
$R-(5)$	$F2(2)$–$F1(2)$	2523.410[b]	3
$R-(5)$	$E(1)$–$E(1)$	2523.410[b]	−3
$R-(5)$	$F1(1)$–$F2(1)$	2523.442	−1
$R-(5)$	$F2(1)$–$F1(1)$	2523.456	1
$R-(6)$	$A2(1)$–$A1(1)$	2528.171	−1
$R-(6)$	$F2(1)$–$F1(1)$	2528.193	1
$R-(6)$	$F1(2)$–$F2(2)$	2528.193	−1
$R-(6)$	$A1(1)$–$A2(1)$	2528.231	−3
$R-(6)$	$F1(1)$–$F2(1)$	2528.245[b]	−1
$R-(6)$	$E(1)$–$E(1)$	2528.245[b]	−5
$R-(7)$	$F2(2)$–$F1(2)$	2532.908	0
$R-(7)$	$E(1)$–$E(1)$	2532.925	1
$R-(7)$	F1(2)–F2(2)	2532.933	−1
$R-(7)$	A1(1)–A2(1)	2532.954	0
$R-(7)$	F1(1)–F2(1)	2533.010[b]	4
$R-(7)$	$F2(1)$–$F1(1)$	2533.010[b]	−3
$R-(8)$	$F1(2)$–$F2(2)$	2537.607[b]	4
$R-(8)$	$E(2)$–$E(2)$	2537.607[b]	−4
$R-(8)$	$F2(2)$–$F1(2)$	2537.634	−2
$R-(8)$	$F1(1)$–$F2(1)$	2537.664	1
$R-(8)$	$E(1)$–$E(1)$	2537.745[b]	6
$R-(8)$	F2(1)–F1(1)	2537.745[b]	3
$R-(8)$	$A2(1)$–$A1(1)$	2537.745[b]	−2
$R-(9)$	$A1(1)$–$A2(1)$	2542.257[b]	3
$R-(9)$	$F1(2)$–$F2(2)$	2542.264[b]	1
$R-(9)$	F2(3)–F1(3)	2542.278[b]	2
$R-(9)$	$A2(1)$–$A1(1)$	2542.305	0
$R-(9)$	$F2(2)$–$F1(2)$	2542.339[b]	3
$R-(9)$	$E(1)$–$E(1)$	2542.339[b]	−4
$R-(9)$	$F1(1)$–$F2(1)$	2542.444[b]	5
$R-(9)$	$F2(1)$–$F1(1)$	2542.444[b]	1

[a] Residuals are given in units of 10^{-3} cm^{-1}.
[b] Blended transition, given a factor of 10 lower weight (see the text).

$$W = \nu_0 + B_3\mathbf{J}^2 - 2B_3\zeta_3\mathbf{J}\cdot\mathbf{l} - D_s\mathbf{J}^4 + F_t O_{ppp3}(\text{tensor}) + Z_t O_{pp33}(\text{tensor}),$$

following Hecht.[23] The values of the molecular constants determined from the simultaneous fitting of the P, Q, and R lines are given in Table V. Allowance was made for the fact that the Q branch has a different effective B_3. Blended transitions were given a factor of 10 lower weight. The relative accuracy of the frequencies of unblended lines was taken to be $\sim \pm 0.002$ cm^{-1}. The estimated precision is approximately correct since the standard deviation is approximately unity (0.85) when taken as

$$\hat{\sigma}^2 = \frac{1}{n_f}\sqrt{\frac{\Sigma_i (y_i - y_c)_i^2}{\sigma_i^2}},$$

where $(y_i - y_c)_i$ and σ_i are the residual and estimated precision of the ith transition frequency, respectively, and n_f is the number of degrees of freedom.

TABLE V. Molecular constants for the ν_3 band of ND_4^+.

	Fitted constants (in cm^{-1})		
$\nu_0 - 2B_3\zeta_3$	2494.042 1(50)[a]	Z_t	$-1.174(10)\times10^{-3}$
$B_3 - B_3\zeta_3$	2.489 06(18)	F_t	$-2.5(16)\times10^{-6}$
$B_3 - B_0(R,P)$	−0.015 146(27)	D_s	$2.92(14)\times10^{-5}$
$B_3 - B_0(Q)$	−0.016 880(36)		
Derived constants [$r_0(NH_4^+) - r_0(ND_4^+) = 0.0020(5)$ assumed]			
r_0	1.0267(5) Å		
B_0	2.9787(29) cm^{-1}		
B_3	2.9636(29) cm^{-1}		
ζ_3	0.1601(9)		

[a] Numbers in parentheses denote three standard deviations in units of the last digits.

Because the available ND_3 was consumed rather quickly, it was not possible to search for forbidden transitions in depth or to measure allowed transitions of higher J. Therefore, the ground state rotational constant B_0 of ND_4^+ can only be estimated at this time. By assuming the same small correction for $r_0(NH_4^+) - r_0(ND_4^+)$ as is known for $r_0(CH_4) - r_0(CD_4)$ we estimate that $r_0(ND_4^+) = 1.0267 \pm 0.0005$ Å and $B_0(ND_4^+) = 2.9787 \pm 0.003$ cm^{-1}. This value of B_0 immediately leads to the values of B_3 and ζ_3 displayed in Table V. The value of ζ_3 is remarkably similar to ζ_3 of CD_4, agreeing exactly within the error limits. When ζ_3 of NH_4^+ and CH_4 are compared, however, it is 10% larger for NH_4^+

As mentioned above, the largeness of ζ_3 for ND_4^+ indicates that the forbidden lines almost certainly cannot be observed with the present sensitivity of our spectrometer. Indeed, it is likely that observation would require orders of magnitude improvement in sensitivity. The determination of $B_0(ND_4^+)$ which this would produce is of interest because it would allow an extrapolation of $r_0(NH_4^+)$ and $r_0(ND_4^+)$ to a somewhat more accurate equilibrium bond distance, r_e. It may be necessary to use other means to arrive at a more accurate value for r_e.

ACKNOWLEDGMENTS

The authors wish to thank B. D. Rehfuss and C. M. Gabrys for assistance in measuring some of the transitions reported in this work. This work was supported by NSF Grant No. PHYS-84-08316 and was also partially supported by the donors of the Petroleum Research Fund administered by the American Chemical Society.

[1]M. W. Crofton and T. Oka, J. Chem. Phys. **79**, 3157 (1983).
[2]E. Schafer, M. H. Begemann, C. S. Gudeman, and R. J. Saykally, J. Chem. Phys. **79**, 3159 (1983).
[3]E. Schafer, R. J. Saykally, and A. G. Robiette, J. Chem. Phys. **80**, 3969 (1984).
[4]T. Nakanaga and T. Amano, Can. J. Phys. (submitted).
[5]Y. Yamaguchi and H. F. Schaefer III, J. Chem. Phys. **73**, 2310 (1980).
[6]A. S. Pine, J. Opt. Soc. Am. **64**, 1683 (1974); **66**, 97 (1976).
[7]Fourier transform spectrum provided by Dr. J. W. C. Johns.
[8]C. Amiot and G. Guelachvili, J. Mol. Spectrosc. **59**, 171 (1976); C. Amiot, *ibid.* **59**, 191 (1976).
[9]D. J. Nesbitt, H. Petek, C. S. Gudeman, C. B. Moore, and R. J. Saykally, J. Chem. Phys. **81**, 5281 (1984).
[10]C. S. Gudeman, M. H. Begemann, J. Pfaff, and R. J. Saykally, Phys. Rev. Lett. **50**, 727 (1983).
[11]M. W. Crofton, W. A. Kreiner, M.-F. Jagod, B. D. Rehfuss, and T. Oka, J. Chem. Phys. **83**, 3702 (1985).
[12]B. D. Rehfuss, M. W. Crofton, and T. Oka, J. Chem. Phys. **85**, 1785 (1986).
[13]J.-E. Lolck, G. Poussigne, E. Pascaud, and G. Guelachvili, J. Mol. Spectrosc. **111**, 235 (1985).
[14]M. A. Thomas and H. L. Welsh, Can. J. Phys. **38**, 1291 (1960); R. A. Olafson, M. A. Thomas, and H. L. Welsh, *ibid.* **39**, 419 (1961).
[15]S. Brodersen, D. L. Gray, and A. G. Robiette, Mol. Phys. **34**, 617 (1977).
[16]S. M. Kirschner and J. K. G. Watson, J. Mol. Spectrosc. **47**, 347 (1973).
[17]G. Tarrago, M. Dang-Nhu, G. Poussigue, G. Guelachvili, and C. Amiot, J. Mol. Spectrosc. **57**, 246 (1975).
[18]C. W. Holt, M. C. L. Gerry, and I. Ozier, Can. J. Phys. **53**, 1791 (1975).
[19]A. Muller, B. Krebs, and S. J. Cyvin, Mol. Phys. **14**, 491 (1968).
[20]K. Kuchitsu and L. S. Bartell, J. Chem. Phys. **36**, 2470 (1962).
[21]Y. Morino, K. Kuchitsu, and T. Oka, J. Chem. Phys. **36**, 1108 (1962).
[22]D. L. Gray and A. G. Robiette, Mol. Phys. **37**, 1901 (1979).
[23]K. T. Hecht, J. Mol. Spectrosc. **5**, 355, 390 (1960).